

END-TO-END ENERGY VARIATION STUDY FOR INDUCTION RADIOGRAPHY ACCELERATOR

Yuan Hui Wu[†] and Yu-Juan Chen

Lawrence Livermore National Laboratory, CA, USA

Abstract

Energy variation study for beam transport from the entrance of a conceptual induction radiography accelerator to the x-ray target has been reported previously [1]. In this report, we have extended the study upstream to the injector. To achieve minimum emittance growth and to obtain a desired final beam size, we have developed three optimal tunes. Among them, one optimal tune, capable of suppressing beam break-up instability and producing acceptable corkscrew motions, is used to study the energy variation effects on radiography performance. The study shows that $\pm 3\%$ energy variation is acceptable.

INTRODUCTION

For a good resolution flash x-ray radiography accelerator, it is desirable to produce small x-ray spots. In this report, we present our study of beam energy variation effects on the final x-ray spot sizes and doses on a 20-MeV conceptual linear induction accelerator (see Fig. 1). Using TRAK [2] ray tracing code and an optimization scheme, we have designed a 2-kA, 2-MV injector capable of delivering a parallel beam (see Fig. 2). The accelerator consists of 72 250-kV accelerating cells, which are grouped in 9 blocks. The downstream section consists of two solenoids and a final focusing solenoid. For simplicity, we assume that there is no target-plasma and back-streaming ions in the target area. Transport from the accelerator to the x-ray converter is modelled with AMBER [3] PIC slice simulations and BREAKUP [4] centroid motion simulations. To achieve desired final spot sizes and minimum emittance growth, several magnetic transport tunes are developed.

TRANSPORTATION OPTIMIZATION

Let $d\gamma/\gamma$ be the A-K gap voltage variation, which leads to the initial beam energy variation, and dV/V be the accelerating cell voltage variation.

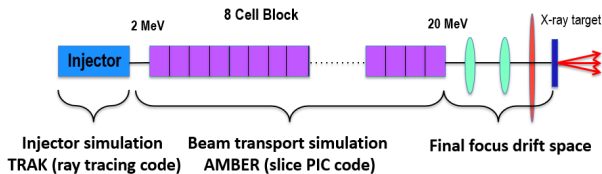


Figure 1: The conceptual accelerator configuration.



Figure 2: A conceptual 2-kA, 2-MV injector.

The nominal beam has no initial energy variation $d\gamma/\gamma = 0$ and does not experience any accelerating voltage variation ($dV/V = 0$). To minimize emittance growth on a space-charge dominated beam, the magnetic tunes are optimized to minimize the nominal beam's envelope. Three optimal magnetic tunes are developed. All three tunes give the normalized emittances at the target around 200 mm-mrad and their final rms spot sizes at about 0.34 mm. Among them, the tune (shown in the top graph of Fig. 3) can suppress the beam breakup instability and provide acceptable corkscrew beam motion is chosen for the energy variation study.

ENERGY VARIATION STUDY

To model energy variation, we assume both the A-K gap voltage waveform and the accelerating voltage waveform have linearly increasing ramps on their tops. For any given A-K gap voltage variation and accelerating voltage variation case, we use 11 voltage values uniformly distributed on the voltage ramps to perform TRAK and AMBER simulations for beam transport of their corresponding 11 beam slices. For this report, $d\gamma/\gamma$ and dV/V is varying coherently from -3% to $+3\%$. These 11 slices' phase spaces at the x-ray converter are combined to form this beam's final time-integrated phase space. We can then use the final time-integrated phase space to calculate the integrated spot size and emittance.

The optimal magnetic tune and 11 slices' rms beam envelopes and normalized Lapostolle emittances are presented in Fig. 3. The curves for the nominal are presented by thick purple lines. As predicted, beam slices with larger energy variations, i.e., accelerated with larger voltage variations, experience larger envelope oscillations, which lead to larger emittance growth.

[†] wu39@llnl.gov

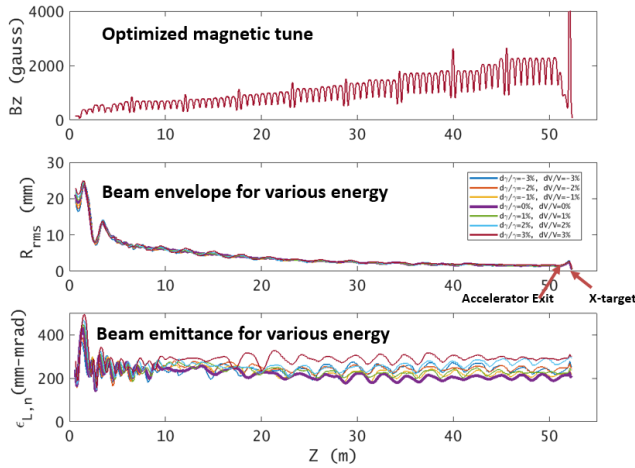


Figure 3: Magnetic tune #2, beam envelopes and emittances for various $d\gamma/\gamma$ and dV/V . The curves for the nominal beam are given by the thick purple line.

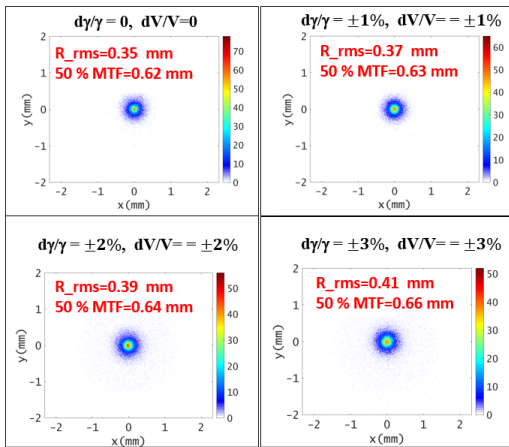


Figure 4: Time integrated x-y spaces at the target for beams with no transverse beam motions.

The time-integrated x-y configurations at the target for beams with $d\gamma/\gamma = dV/V = 0, \pm 1\%, \pm 2\%$, and $\pm 3\%$, are presented in Figs. 4. The calculated time-integrated rms beam radius and 50% Modulation Transfer Function (MTF) [5] spot size are given in the figure for each energy variation. The time-integrated phase spaces and normalized Lapostolle emittance at the target for these energy variations are presented in Fig. 4.

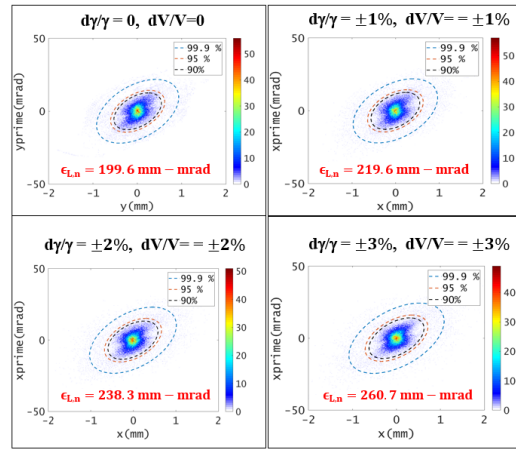


Figure 5: Time integrated phase spaces at the target for beams with no transverse beam motions.

BEAM MOTIONS AND SPOT SIZE

The transverse beam motions with $d\gamma/\gamma = 0 - \pm 3\%$ and $dV/V = 0 - \pm 3\%$ are modelled with BREAKUP code. The beam is initial offset by $x_{\text{off}} = y_{\text{off}} = 0.5$ mm. The 3σ of the system's solenoid displacement is 2 mm, and the 3σ of the solenoid tilts is 2 mrad.

To calculate the final spot size and emittance for each energy variation case, we project the physical spaces and phase spaces of the beam's 11 slices on the time-integrated physical space plane and phase space plane with their corresponding transverse displacements. Then, the spot size and emittance are calculated based on the time-integrated physical and phase spaces. The effected x-ray dose changes using the scaling law in Ref. [6] are estimated also.

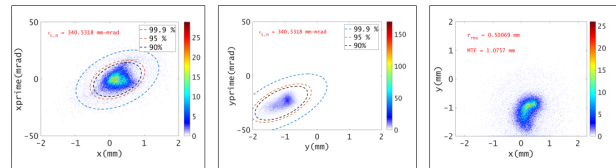


Figure 6: Time-integrated x-x' and y-y' phase spaces and spot size at the x-ray target with transverse beam motions without any steering.

For the beam having $\pm 3\%$ energy variation, the amplitude of its centroid motion without steering is about 1 mm. Its time-integrated x-x', y-y' and x-y spaces are shown in Fig. 6. Comparing them with the time-integrated physical space and phase space shown in Figs. 4 and 5, it is clear that its large transverse beam motions have made its time-integrated spot size and emittance larger.

The beam centroid motions can be reduced after implementing a steering optimization using global optimization algorithm (genetic algorithm). After the steering, the time-integrated x-y configurations and phase spaces at the target for beams with $d\gamma/\gamma = dV/V = 0, \pm 1\%, \pm 2\%$, and $\pm 3\%$, are presented in Figs. 7 and 8.

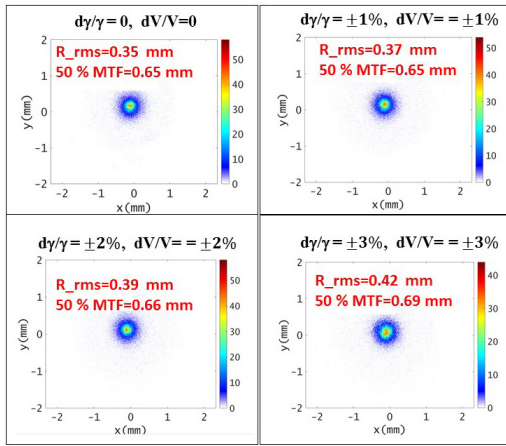


Figure 7: Time integrated x-y spaces at the target for beams with transverse beam motions and with steering.

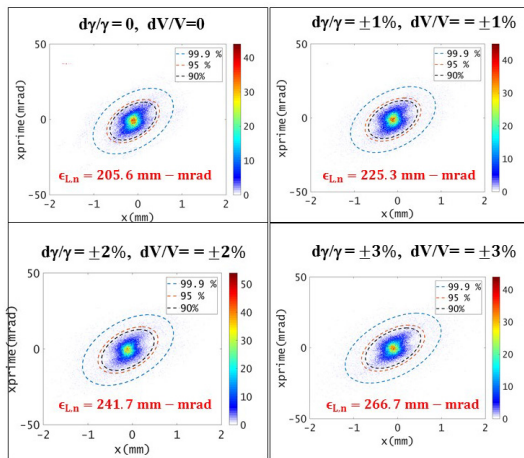


Figure 8: Time integrated phase spaces at the target for beams without transverse beam motions with transverse beam motions and with steering.

The calculated spot sizes, emittances and x-ray dose changes based on the time-integrated physical and phase spaces in Figs. 7 and 8 are presented in Table 1. The results indicate that accelerator with up to $\pm 3\%$ voltage variation has only small effects on the spot sizes and the forward x-ray dose.

SUMMARY

We have studied the effects of beam energy variation on a conceptual radiography accelerator's performance numerically. The end-to-end electron beam transport is optimized for minimum emittance growth and for achieving a desired spot size at the x-ray converter. For each beam slice with a different energy, beam transport in the injector is simulated with TRAK ray tracing code. Beam transport on the rest of the machine is simulated with AMBER PIC code and BREAKUP centroid code. The results show that the beam energy variation up to $\pm 3\%$ only weakly affects the time-integrated 50% MTF spot size and forward x-ray dose.

Table 1: Summary of Beam Parameters at the Target with Transverse Beam Motion and with Optimal Steering

Injector energy spread (\pm %)	Accelerator Voltage variation dV/V (\pm %)	R_{rms} (m)	Normalized Lapostolle Emittance (mm-mrad)	50% MTF (mm)	dD/D (%)
0	0	0.35	205.6	0.648	0
1	1	0.37	225.3	0.655	0.30
2	2	0.39	241.7	0.659	0.59
3	3	0.42	266.5	0.689	1.18

ACKNOWLEDGEMENTS

The authors would like to thank Jennifer Ellsworth for useful discussions. This work was performed under the auspices of the U.S. Department of Energy by Lawrence Livermore National Laboratory under Contract DE-AC52-07NA27344.

REFERENCES

- [1] Y. H. Wu *et al.*, LLNL-CONF-703942, NA PAC, Chicago, IL, 2016, pp. 1-2.
- [2] Field Precision LLC. © 1998 – 2017.
- [3] J. L. Vay, W. Fawley, Amber code, 2000.
- [4] Y-J Chen, W. Fawley, Breakup Code.
- [5] Joseph W. Goodman, *Introduction to Fourier Optics*, Third edition, 2004, Roberts and Company publishers.
- [6] Y-J Chen, April 2000. UCRL-ID-140189, LLNL, pp. 1-2.